Article:
Mateus Tarazona, D, Prieto, JA, Murphy, W orcid.org/0000-0002-7392-1527 et al. (1 more author) (2021) Identification of submarine landslides in the Colombian Caribbean Margin (Southern Sinú Fold Belt) using seismic investigation. Leading Edge, 40 (12). pp. 914-922. ISSN 1070-485X

https://doi.org/10.1190/tle40120914.1

IDENTIFICATION OF SUBMARINE LANDSLIDES IN THE COLOMBIAN CARIBBEAN MARGIN (SOUTHERN SINÚ FOLD BELT) USING SEISMIC INVESTIGATIONS

Darwin C. Mateus[1, 3], Jorge A. Prieto[1]. William. Murphy[2], Julian F. Naranjo[3]

[1]*Department of Civil Engineering, EAFIT University.*

[2]*School of Earth and Environment, University of Leeds, Leeds, LS2 9JT, United Kingdom.*

[3]*Ecopetrol S. A.*

ABSTRACT

Submarine landslides can be triggered by several processes and involve a variety of mechanisms. These phenomena are important sediment transport processes but also constitute a significant geohazard. Mapping of the southwestern Caribbean Sea using 3D seismic data has allowed the identification of several submarine landslides in the Colombian Margin in the area dominated by the Southern Sinú Fold Belt (SSFB). A post-tack depth-migrated seismic cube survey with a 12.5 m by 12.5 m bin spacing was used to identify landslides in an area covering 5746 km^2. Landslides were interpreted using: a seafloor morphologic parameter identification process; and the internal deformation of the slope forming material, as seen from seismic data. A total of 93 landslides were identified and classified based on their movement styles, as follows: 52 rotational, 29 translational, and 12 complex landslides. In addition, 12 distinct deformational zones, and a zone of Mass Transport Complex (MTCs) were identified. Five different ground condition terrain were interpreted based on landslides type and distribution as well as in geological structures and seismic reflection analysis. Two main processes seem to influence landslides in the study area. First, the folding and faulting involved in the Southern Sinú Fold Belt (SSFB) evolution. This process results in oversteepened slopes that starts as deformational zones and then fail as translational or rotational slides. Those individual landslides progressively become complex landslides zones that follow geological structural orientation. Second, the continental shelf break erosion by debris flows which fill in intra-slope subbasins and continental rise with several MTCs. According to the results, risk of damage by landslides increases in distances shorter than 4 km along structural ridges foothills in the whole study zone.

INTRODUCTION

Submarine and terrestrial landslides are mass movements occurring downslope due to a mechanical failure (Cruden and Varnes, 1996). Undersea, these phenomena play an important role shaping morphological features and transporting sediment on continental margins (McAdoo et al., 2000; Masson et al., 2006). They are also important trigger mechanisms for tsunamis and avalanche generation (Nadim et al., 2006; Vanneste et al., 2013; Leslie and Mann, 2016; Heidarzadeh et al., 2019).

The usual definition of landslide i.e. downward and outward movements of soil, rock or some combination of the two, which has clearly defined boundaries at top, bottom, sides and base,

can be enlarged for the submarine environment. In the marine environment, landslides classes include whether landslides are frontally constrained (namely the slide mass still sits at least partially within its boundaries) or frontally unconstrained (the sliding mass has completely vacated the landslide scar). A variety of classifications exist for subaerial and submarine landslides (Shanmugam and Wang, 2015). This study adopted the classification suggested by Cruden and Varnes, (1996) in which landslides processes include translational landslides, rotational landslides, and debris flows. Mass Transport Complex (MTCs) is used to describe deposits where the mechanism of emplacement is unclear (Moscardelli et al., 2006; Moscardelli and Wood, 2016). Additionally, the term Deformational zone is utilized to refer to potential landslide zones where a mass movement is ongoing, but where boundaries cannot be clearly defined and where there are no fully formed shear surfaces.

Submarine landslides and MTCs have been studied worldwide in different geological settings (Hampton et al., 1996; McAdoo et al., 2000; Green and Uken, 2008; He et al., 2014; Lamarche et al., 2016; Shanmugam, 2016). Consequences of submarine landslides can be significant in terms of loss of life (Tappin et al., 2001), damage to coastal infrastructure (Carter et al., 2012) and for the Oil and Gas industry where the costs can reach about US$ 400 million annually (Lamarche et al., 2016).

In the Colombian Caribbean margin, research has been focused on landslide processes and MTCs mainly associated with the Magdalena fan (Romero-Otero, 2009; Ortiz-Karpf et al., 2017; Idárraga-García et al., 2019). Research has also highlighted the significance of submarine landslides as geohazards for offshore infrastructure (Alfaro and Holz, 2014a; Leslie and Mann, 2016). However, research has addressed the geomorphological characterization of the sea floor in detail in order to identify potential submarine slopes instabilities. In this document the geomorphological mapping of landslides using high resolution 3D Seismic survey is described as are the descriptive statistics of those landslides. Geophysical data are used to identify both geomorphological features on seafloor and sub-surface internal pattern to define both the landslide morphology and deformation characteristics. This combination of observations has allowed the expected type and average size of future landslides in the study zone to be inferred and gives insights for landslides generation processes in the Colombian Caribbean margin.

Regional setting

The study area (Figure 1) is located in the south west of the South Caribbean Deformed Belt (SCDB), in a zone dominated by the Southern Sinú Fold Belt (SSFB) (Martinez et al., 2015) which is classified as an Accretionary Prism (Ruiz et al., 2000; Bernal-Olaya et al., 2015) and extends from the Urabá Gulf, in the South, to the Santa Marta Offshore region in the North (Flinch et al., 2003).The SCDB is the product of the obliquely collision between the Caribbean plate and the North Andes Plate (Pindell, 1994; Martinez et al., 2015). The Caribbean plate moves easterly and is subducted beneath the North Andes plate (Pindell, 1994; Symithe et al., 2015). This creates a stress field in the Southwest Caribbean resulting in a strike-slip faulting as well as compressional zones (Bird, 2003; Rodríguez et al., 2021). Moreover, the southern part of the study area is also

affected by the North-eastern Panama plate movement, which is forming the Panama Fold Belt (PFB) (Alfaro and Holz, 2014a) and the Uramita fault (Figure 1).

Data collection and analysis

The area under investigation covers a significant range of bathymetry and different geomorphological settings, i.e. from continental slope to continental rise. Intra-slope subbasins and structural ridges are most representative morphology in continental slope while MTCs, canyons and abandoned channel systems cover the continental rise (Rincón et al, 2021). The primary data used in this investigation was a post-tack depth-migrated seismic cube survey (PSDM) which covers an area of 5,743 km^2. Sample rate was 2 milliseconds (ms) and the recording length was 15,000 ms with a receiver interval of 12.5m. Seismic cube has a bin spacing of 12.5 m by 12.5 m.

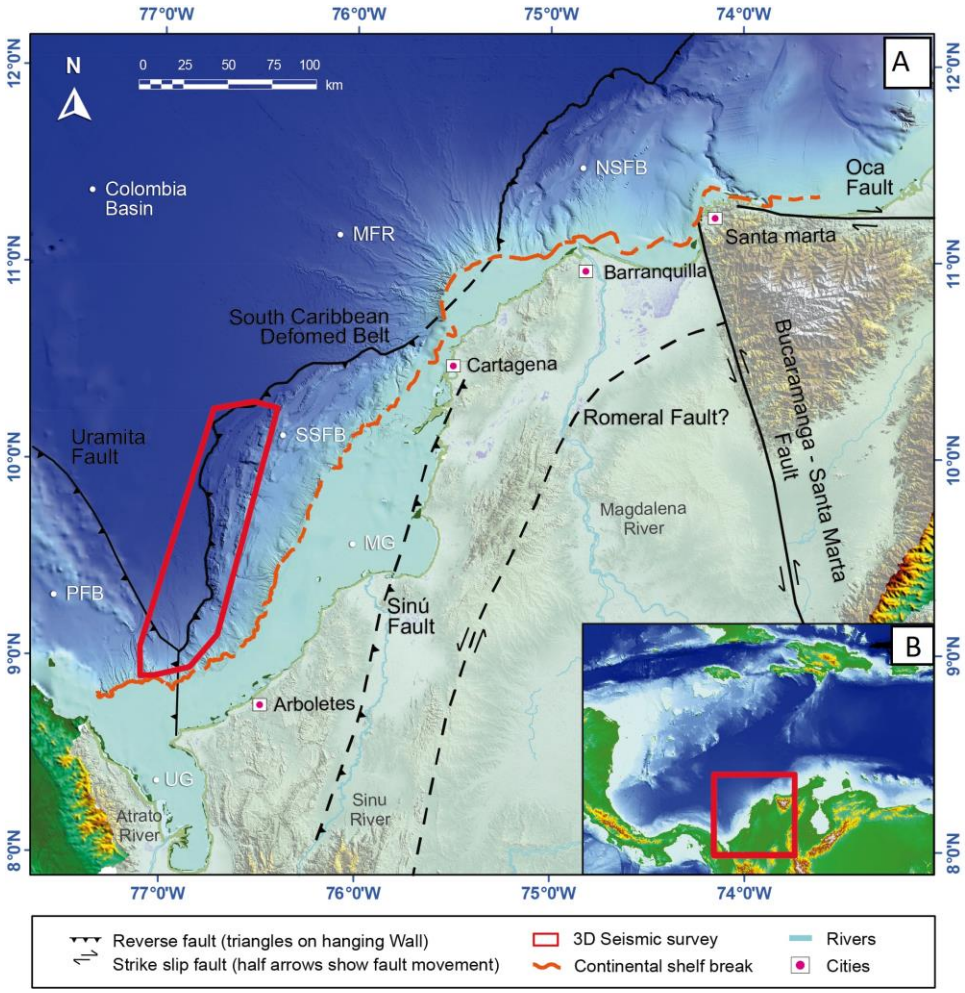

Figure 1. a) Topographic and Bathymetric map of the Northwest of Colombia showing the study zone (red polygon) and main geological features (Rincón et al, 2021). The South Caribbean Deformed Belt is locally divided in the North Sinú Fold Belt (NSFB), Magdalena Fan River (MFR) and the South Sinú Fold Belt (SSFB) (Martinez et al., 2015). It is also included the Panama Fold Belt location (PFB) (Alfaro and Holz, 2014a) The Golf of Morrosquillo (MG) and the Urabá Golf (UG). b) The red box shows the location of the enlarged information in panel A. Modified from Rincón et al, (2021)

First step for identifying submarine landslides on the study area was to obtain the sea floor surface based on the seismic cube. To accomplish this purpose, the first strong reflector was followed to generate a continuous surface. Then, seismic reflection changes on amplitude, dip and continuity as well as geomorphological features were used to identify landslides (Shanmugam and Wang, 2015; Shanmugam, 2016). The main characteristics that were used for slide identification were: the crown, significant scarps and the geometry of the displaced mass as outlined by He et al., (2014). Somewhat more challenging were features which had the geometry of landslides but the body of the landslide was absent indicating that the slide mass had vacated the landslide scar.

Types of Landslides were defined based on its kinematics (Cruden and Varnes, 1996). Thus:

1) Transitional slides, i.e. planar failure surface, for example along a planar bedding planes. 2) Rotational slides characterized by circular slip surfaces and internal deformation. 3) Complex landslides in which a lateral or vertical superposition of more than one slide masses with different movement mechanisms were identified.

TERRAIN CLASSIFICATION AND LANDSLIDE IDENTIFICATION

On the basis of seafloor geomorphology, seismic reflection features and landslide occurrence, it was possible to define five terrain types (Figure 2a) with characteristics as summarises in Table 1.

Landslides

In total were identified 93 landslides, 12 deformational zones, and a zone controlled by Mass Transport Complexes (MTCs) besides several mud volcanos (Figure 3). Features were grouped in 52 rotational, 29 translational, and 12 complex landslides. This research took into account quantitative morphological parameters suggested by Clare et al., (2018) which include: total landslide length (Lt), scar perimeter length (Ls), scar width (Ws), total height drop (Ht), slope gradient (S), slope gradient of the heads carp (Ss), area and volume (Figure 4b-d).

Rotational slides.

Rotational slides are characterized by a circular slip surface which cut continuous seismic reflections from unaltered material. Highly-deformed, semi continuous to discontinuous seismic facies can be observed within displaced mass. Most of the rotational slides identified are located on oversteepened slopes associated with imbricated thrusts and reverse faults. Figure 4 shows an example which is influenced by a Northeast - Southwest strike-slip fault and by a structural ridge which confine its displaced mass obliquely to the crown. Its horizontal extent (Lt) is 12.5 km and 5.92 km scarp width. In general, minimum area covering rotational landslides is 0.24 km^2 while maximum area is 52 km^2. However, in 30 of the 52 rotational slides was not possible to estimate this parameter since the displaced mass was vacate.

Table 1. Summary of terrain type characteristics.

Terrain Unit	Name	Seismic characteristics	Geomorphological characteristics	Landslide data
T1	Magdalena fan deposits (MFD)	Characterized by flat-lying high-amplitude continuous coherent seismic reflections.	Slope angle in this zone is normally less than 2 degrees and dominated by sedimentation by gravity. The buried channels in section without evidence of surface erosion.(Figure 2b)	No evidence of landslides on this terrain unit.
T2	Colombian basin, domain of MTCs (CB-MTCs).	Sub-horizontal low-amplitude to steeply-dipping chaotic reflections.	Interplate zone showing little or no evidence of compressional tectonics. Superposition of mass transport deposits is evident. (Figure 2c)	Only evidence of the deposits of landslide activity generated from zone 3. Occasional large blocks can emerge from MTCs and be carried into Zone 1.
T3	Southern Sinú Fold Belt (SSFB)	Parallel continuous to discontinuous high amplitude reflections	Seafloor surface is characterized by imbricated folds and high angle reverse faulting which allow the filled of several intra-slope basins. (Figure 2d)	The majority of landslides observed occur in this area. The oversteepening caused by reverse faulting is a significant trigger.
T4	Urabá basin – domain of MTCs (UB-MTCs)	Oblique to discontinuous low amplitude reflectors	Smooth bathymetry with development of gullies and canyons and mud volcanos. Subsurface characterized by folds and high angle reverse faulting (Figure 2e)	Rotational Landslide and slide scar are observed on canyon wall
T5	Southern Sinú Fold Belt (SSFB) – domain of MTCs (SSFB-MTCs)	Sub-horizontal low-amplitude chaotic reflections	Seafloor surface presents hummocky morphology. Subsurface characterized by overfilled intra-slopes basins. (Figure 2f)	Debris flows scars are main landslides observed on seafloor surfaces.

Translational slides.

Translational landslides are characterized by a largely planar-failure surface on which displaced mass moves. In the study zone, landslides of this type are associated with structural ridge limbs (Figure 5). Either thin masses were present or the displaced masses had vacated the landslide boundaries, therefore, it was impossible to estimate total length distance (Lt) and other morphometric parameters depending on displaced mass on 20 of the 29 landslides. For those landslides which allowed measurements, the minimum area covering was 0.38km^2 while the maximum area was 10.87 km^2. Minimum and maximum total length (Lt) observed was 0.65 km and 1.92 km respectively.

Complex Landslides.

Complex landslides are formed by superposition of lateral or vertical landslides (Hampton et al., 1996; He et al., 2014) and can involve one or both translational and rotational kinematics. In the study area they are associated with regional reverse faulting. Seismic facies vary from lightly disturbed reflections to highly bonded discontinuous reflections (Figure 6). Maximum estimated area was 209 km^2 and volume of 108 km^3.

Deformational zone.

Deformational zones are characterized by discontinuous parallel seismic reflections with low to moderate amplitude, which are seen to be affected by normal faulting with small offsets (Figure 7). These zones are located mainly on structural ridge limbs and are associated with landslides scarp perimeters. The normal faults evident in this zone do not extend the full depth of the seismic section and tend to terminate against clear reflectors. It seems likely that these are progressive slide blocks which have not yet developed into large scale failures of the submarine slope. This, to some extent, would fit the geographic relationship between slide scars and scarps.

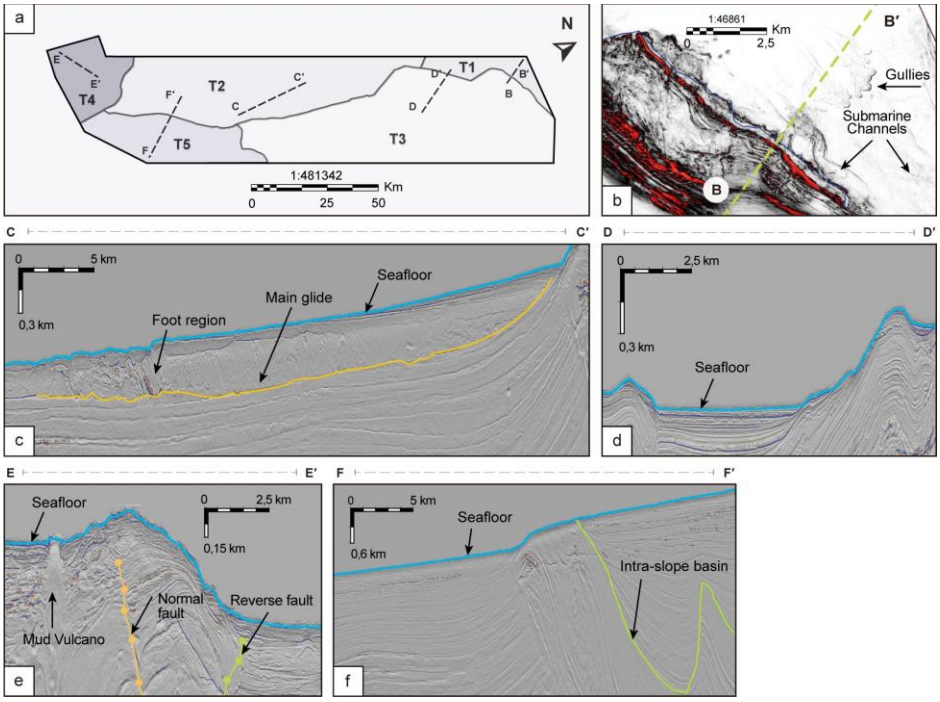

Figure 2. Terrain types. a) Distribution Plan view of the five terrain types. b) Time slide of variance seismic attribute showing abandoned gullies and channels as main morphological characteristic of terrain type T1, white color means low variance (flat reflectors) whereas red color means high variance on seismic signal. c) Seismic section showing Mass Transport Complex (MTC) on Terrain type T2. Low amplitude and semi-continuous reflections are a characteristic of syndepositional trusts on foot region. Blue line represents seafloor. d) Overstepped slopes that fail and fill intra-slope basin in terrain type T3. e) Terrain type T4, lime and amber lines represent faults related to the Uramita fault system. f) Terrain type T5 green line represents the base of an intra-slope basin which is filled by MTCs characterized by low amplitude and semi-continuous reflections.

Mass Transport Complexes (MTC).

Mass transport complexes are deposits of multiple, potentially large, landslides whose scars are unidentified. They present as inter-bedded packages filling intra-slopes basins in terrain type T3 and as the main sedimentation process in terrain type T2 and T5. Figure 8 presents the largest MTC observed in the study zone, it is 64 km horizontal length, 12 km width, maximum deposit thickness of 0.6 km covering an area of nearly 700 km^2 and a volume of 51 km^3. Its basal surface is irregular and presents scours northeast oriented and erosive boundaries. This large MTC induces pressure ridges on seafloor perpendicular to its movement direction.

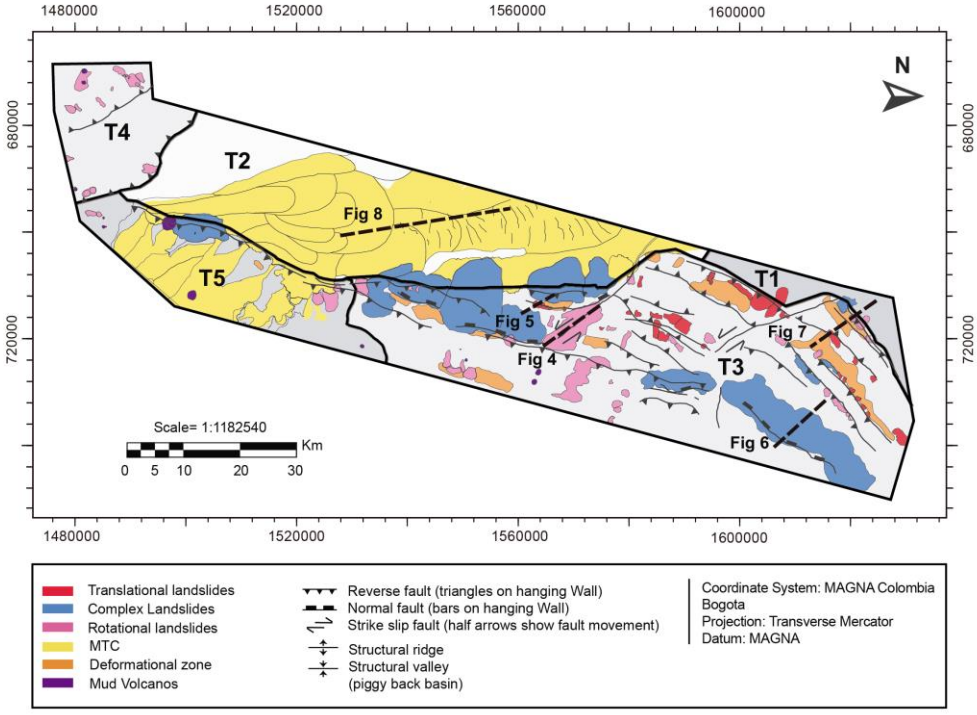

Figure 3. Geographic distribution of submarine landslides in the study zone. Yellow areas represent Mass Transport Complex (MTC). Blue areas represent complex landslides, red areas represent translational slides, magenta areas represent rotational slides, orange areas represent Deformational zones, and purple areas represent mud volcanos. T1 to T5 represent terrain types and long dashed black lines show the location of Figures 4 to 8.

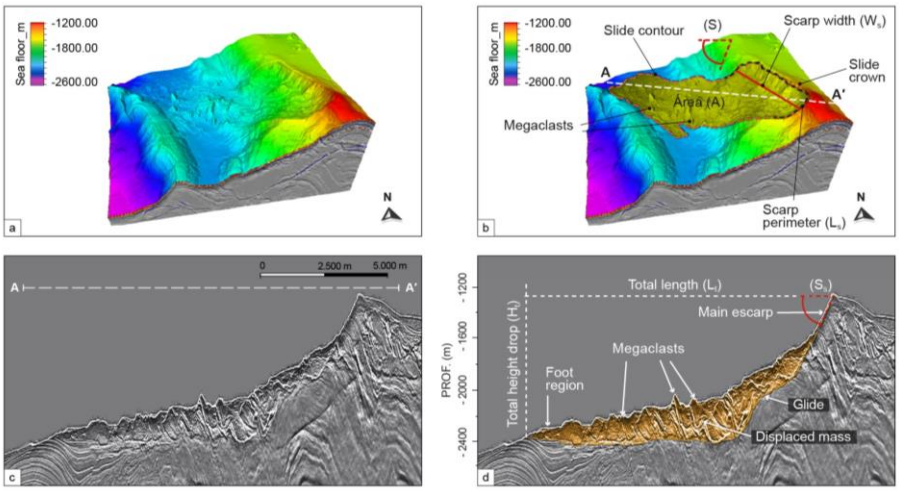

Figure 4. Rotational landslide. a) Tridimensional view of seafloor surface without interpretation. b)Tridimensional view of a rotational landslide (RS5 in Appendix 1) showing morphological characteristics on seafloor like megaclasts, slide crown and slide contour. This panel also show the Scar perimeter length (L_s), scar width (W_s) and slope gradient. (S) in a typical landslide. c) Seismic section without interpretation. d) Seismic section showing main landslide characteristics like failure plane (glide), Displaced mass internal deformation (Copper area), megaclasts food region, total length (L_t), total height drop (H_t) and slope gradient of the heads carp (S_s). Modified from Rincón et al, (2021)

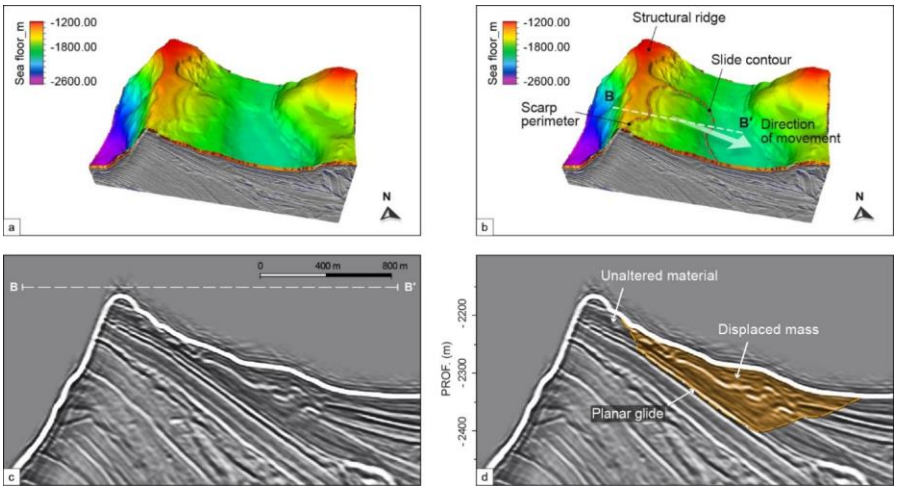

Figure 5. Translational slides. a) Tridimensional view of seafloor surface without interpretation. b) Tridimensional view of a translational slide highlighting slide contour, direction of movement and Scarp contour. c) Seismic section without interpretation. d) Seismic section showing landslide displaced mass (Copper area) planar glide that moves parallel to bending planes and displaced mass internal deformation. Modified from Rincón et al, (2021)

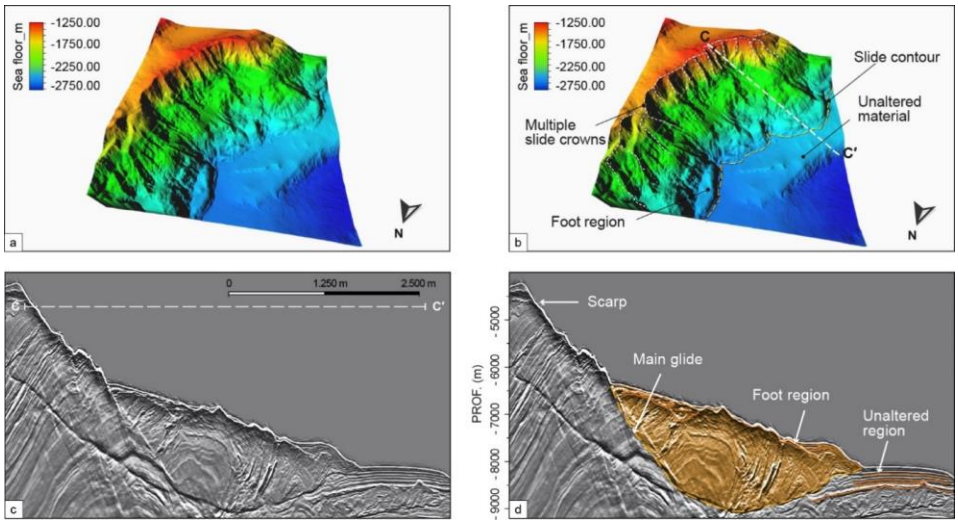

Figure 6. Complex Landslide. a) Tridimensional view of seafloor surface without interpretation. b) Tridimensional view of a Complex landslide where multiple slide crown, foot region and slide contour are showed. c) Seismic section without interpretation. d) Seismic section of the complex landslide. Copper colored area highlights displaced mass on main glide. Foot region is characterized by folding and reverse faulting as a result of the lateral movement. Unaltered region presents parallel and continuous seismic reflectors at the right side of the landslide. Modified from Rincón et al, (2021)

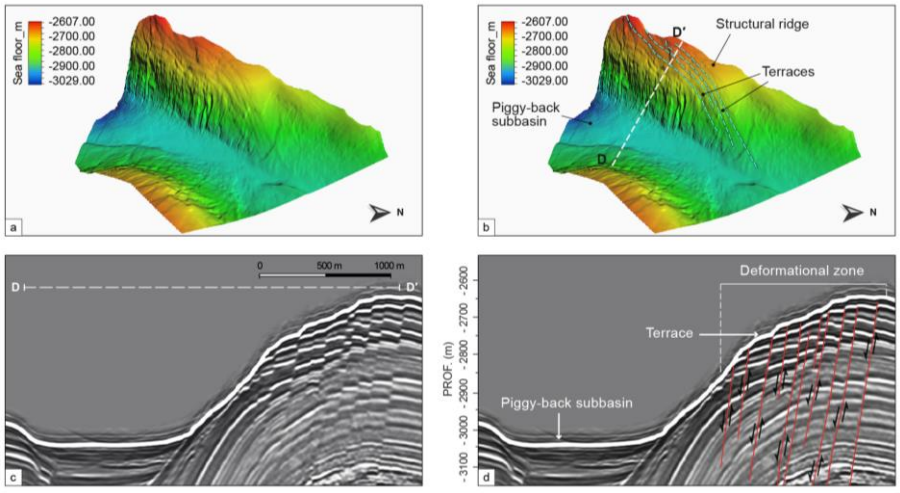

Figure 7. Deformational zone. a) Tridimensional view of seafloor surface without interpretation. b) Tridimensional view of a deformational zone showing terraces resulting of small drops by normal faulting (Jungle green dashed line). c) Seismic section without interpretation. d) Seismic section of the deformational zone highlighting, terraces and normal faulting. Reflectors discontinuity suggest lack of strength in the structural ridge limb which could trigger new landslides in the future. Modified from Rincón et al, (2021)

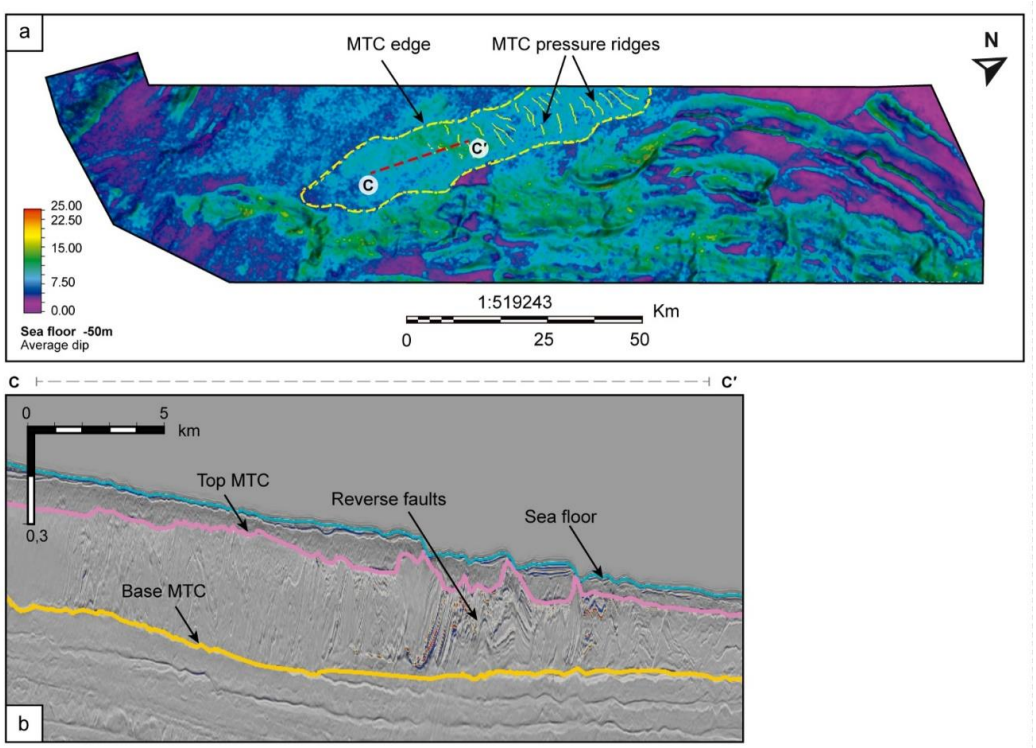

Figure 8. MTC. a) Average dip attribute calculated 50m under seafloor highlights the MTC contour. b) Interpreted limits of the MTC in Cross section C-C' showing low amplitude, semi-continuous reflections as a characteristic of syndepositional compression. Orange line represents the base of the main movement. Magenta line represents the top of the mass movement event.

Statistics of individual landslides

Figure 9 shows a general view of landslides size. According to this, it is clear that complex landslides and MTCs are significantly larger than individual events, the formers involve tens of kilometers of scarp width and horizontal movement, while most of the individual events present less than 6 km of scarp width and horizontal movement less than 10 km. "Appendix A" presents morphologic parameter measured for all landslides interpreted in the study zone.

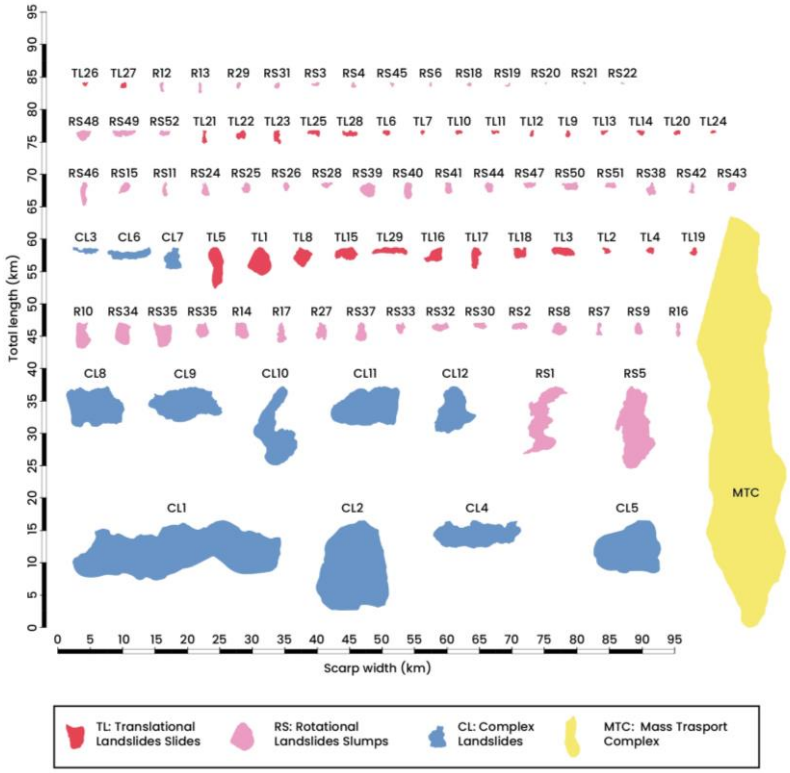

Figure 9. Plan view of landslide oriented toward movement direction. Yellow polygon represent a MTC, blue polygons represent complex landslides (CL), magenta polygons represent rotational slides (RS), and red polygons represent translational slides (TL). Horizontal movement – Total length (Lt) is graphed in vertical axe and scarp width (Ws) is represented on the horizontal axe of the figure.

Figure 10 shows frequency histograms for main morphometric parameter of 31 individual landslides. Complex landslides and MTC zones were exclude from this analysis since they involve more than one slide event. Additionally, individual landslides in which displaced mass was vacate from de scar were also excluded. Maximum and minimum total height drop (Ht) found was 1.18 km, and 0.094 km respectively with a mean value of 0.4 km and a standard deviation of 0.240 km. Maximum total length (Lt) reached was 12.5 km in RS5 and the minimum value was 0.54 km in RS22. However, 93% of data (29 landslides) showed Lt less than 4 km. Maximum scarp width observed was 5.9 km and the minimum one was 0.37 km, 90% of the data (28 Slides) showed scarp width less than 2.4 km. Minimum and maximum Slope angle of head scarp (Ss) was 8 and 44 degrees respectively, with an average of 26 degrees, while near to landslides, minimum and maximum non-failed slope angle (S) was 5 and 25 respectively. Minimum volume of individual

landslides was 0.004 km^3 and maximum 8.54 km^3, however 90% of the data was lower than 0.16 km^3.

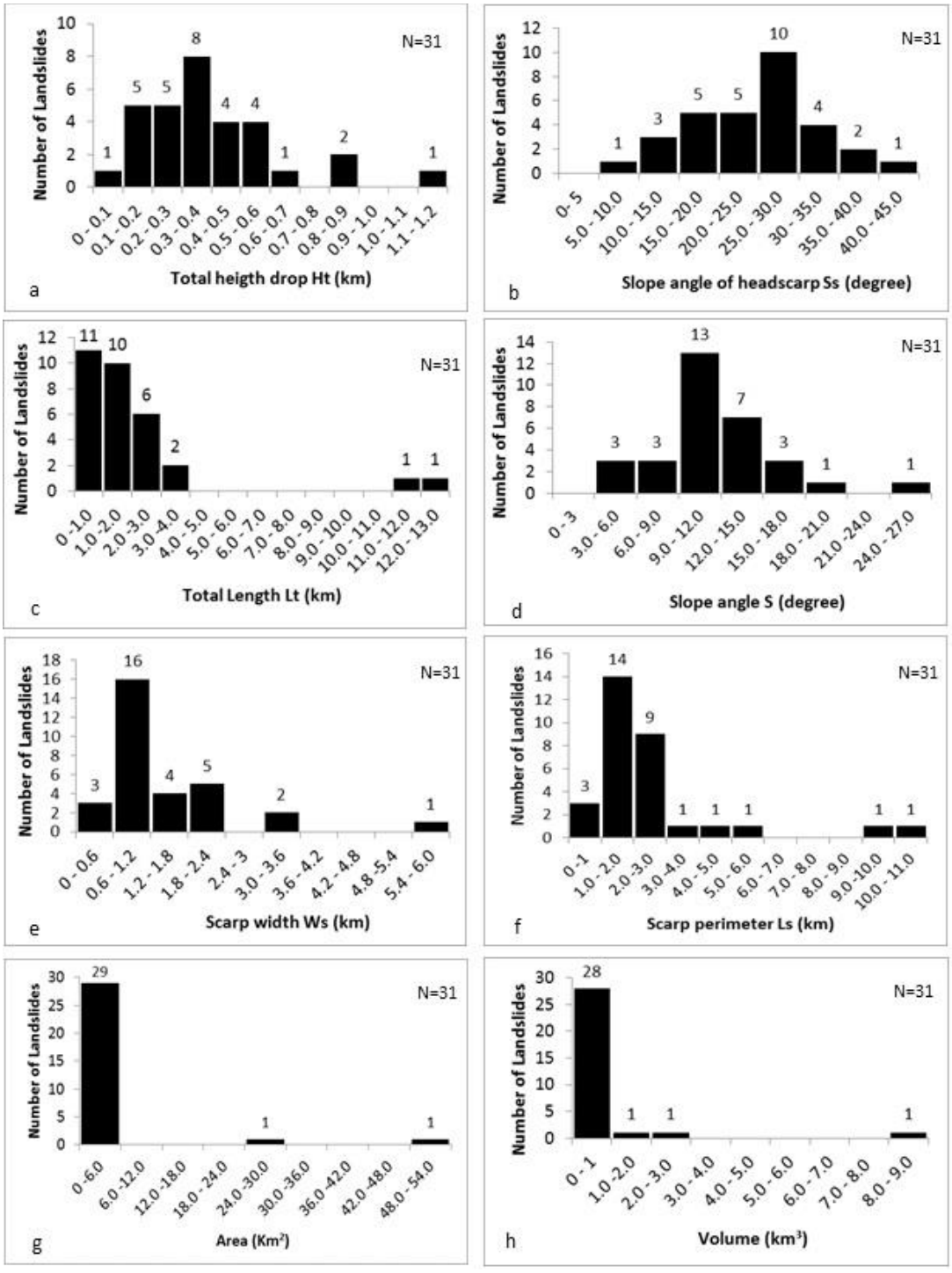

Figure 10. Frequency histogram of morphologic parameter for individual landslides. a) Total height drop (Lt). b) Slope angle of head scarp (Ss). c) Total length (Lt). d) Slope angle (S). e) Scarp width (Ws). f) Scarp perimeter (Ls). g) Area. h) Volume.

Table 2. Shows correlation coefficient between landslides morphometric parameters. Good correlation is evident between Total length (Lt), Total height drop (Ht), Scarp width (Sw) and volume. Those relations has been documented worldwide (Hampton et al., 1996; McAdoo et al., 2000; Green and Uken, 2008; He et al., 2014). Correlation between Sw and Lt is certainly useful since it gives the possibility to estimate the maximum distance reached by new landslides through mapping possible crowns on deformational zones.

Table 2. Correlation coefficient between landslides morphologic parameters. Ht - Total height drop. Lt -Total Length. Ws - Scarp width. Ls - Scarp perimeter length. Ss - Slope gradient of head scarp. S - Slope gradient. Vol - Volume.

	Ht	Lt	Ws	Ls	Ss	S	Vol	Area
Ht	1,00							
Lt	0,74	1,00						
Ws	0,70	0,75	1,00					
Ls	0,66	0,85	0,83	1,00				
Ss	0,20	0,00	-0,01	-0,18	1,00			
S	0,02	0,18	0,08	0,12	-0,03	1,00		
Vol	0,68	0,82	0,79	0,71	0,02	0,20	1,00	
Area	0,75	0,94	0,85	0,85	-0,01	0,17	0,95	1,00

DISCUSSION

The distribution and characteristics of submarine landslides and MTCs in the study area show a clear association with ground condition, which in turn respond to the combination of tectonic deformation and sediment supply (Rincon et al., 2021). For this reason, our interpretation of the connection between subsurface conditions and observed landslides and MTCs is presented below. Similarly, main processes that we believe are controlling the occurrence of submarine landslides in this convergent margin zone are argued. This will contribute to understand submarine landslides generation in this type of geological environment.

Relation between terrain types and Landslides

In Terrain T1, the absence of observable landslides would suggest that this terrain type is a low landslide risk area. The slow slope angle in the bathymetry (<2°) is the result of the high rate of sediments supplied by the Magdalena River that feeds channel-levees, in the continental slope, and smooth the marine relief in the abyssal basin (Flinch et al., 2003; Naranjo-Vesga et al., 2020).

Terrain T2 is the result of two effects: the inter-plate tectonics associated to the collision along the North Andes plate and the Caribbean plate; high sedimentation rates supplied by mass transport events, originated in the continental shelf break. These events feed Mass Transport

Complexes (MTCs) that show hummocky appearance (Vanneste et al., 2013) and compressional ridges on seafloor. Rarely translational or rotational slides are present on surface except by those located near foothills which are originated in terrain type T3.

Most of the landslides observed are located in the Terrain T3 (SSFB) which is the result of the collision between the North Andes continental plate and the Caribbean oceanic plate (Ruiz et al., 2000; Martinez et al., 2015; Rodríguez et al., 2021). Translational slides occur mainly in structural limbs where bedding dip concur with the seafloor slope (Figure 5). Whereas individual rotational slides seem to be present in two geological context. First, structural limbs where bedding dip is in opposite direction to the seafloor slope. Second, in canyon walls that cut geological structures both in T3 and T4. Complex landslides formed by the succession of lateral translational slides are present at the North part of the study zone and involves thin beds along structural limbs (CL3, CL6, CL7 in Figure 9). On the other hand, larger complex landslides, showing a rotational kinematics are associated with main structural ridges and faults that forms the SSFB. (Figure 3). They involve both recent sediments and compacted rocks exposed by reverse faulting. Consequently, coherent movement of rotational landslides are observed (Figure 6).

Terrain T5 seabed is characterize by Mass Transport Complex (MTCs) which are interpreted as a result of multiple debris flows originated at the continental shelf break (Figure 1). The seabed scours reported by Alfaro and Holz, (2014a) and Rincon et al, (2021) allow us to infer that debris flows are the main feeder source of MTCs in this zone. These debris flows are deposited downward filling intra-slope subbasins throughout the continental shelf and eventually reaching the continental rise.

Landslides processes

Two main processes influence landslides in the study area. First, the folding and faulting involved in the Southern Sinú Fold Belt (SSFB) evolution. This process results in oversteepened slopes that starts as deformational zones (Figure 11a) and then fail as translational (Figure 11b) or rotational slides (Figure 11c). Second, the continental shelf break erosion by debris flows which fill in intra-slope subbasins and continental rise with several MTCs (Figure 11d).

MTCs involve areas of hundreds of square kilometers and tens of cubic kilometers in volume. In terrain T3 these deposits partially fill intra-slope subbasins which avoid MTCs to reach the continental rise, while in terrain T5, MTCs have overfilled intra-slope subbasins, allowing them to travel from the continental shelf break to the continental rise, in terrain T2 (Figure 3). MTCs observed in the seismic record are interpreted as a result of multiple landslides events, as a consequence, must not be interpreted as instantaneous events for geohazards assessment purposes, because it could overestimate volumes involved in mass movements.

The most important features in terms of triggering future landslides are deformational zones in the limbs of structural ridges in terrain T3 (Figure 3) since they involve failed material in a preconditioning stage (Vanneste et al., 2013). These zones cover areas between 1.48 and 47.6 km^2 identified as slopes with angles between 5° and 15° which is also the slope angle interval where more landslides occur (Figure 10d).

Some of the landslides showed just the vacated scars (not the displaced masses). Therefore, it was cumbersome estimate maximum horizontal total landslide length. However, following the morphological parameters statistical data (Table 2), and the good correlation coefficients (~0.75) between scarp width, Ws, and total landslide length, Lt, yielding Ws=0.75 Lt, we estimated total lengths from measurements of scarp width in 81 landslides. Average total landslide lengths in the order of 3 km were obtained. Consequently, we argue that individual landslides in the study zone should have total lengths less than 4 km. Note that total landslide length can have relevance for geohazards assessments because offshore infrastructure can be affected by landslides size.

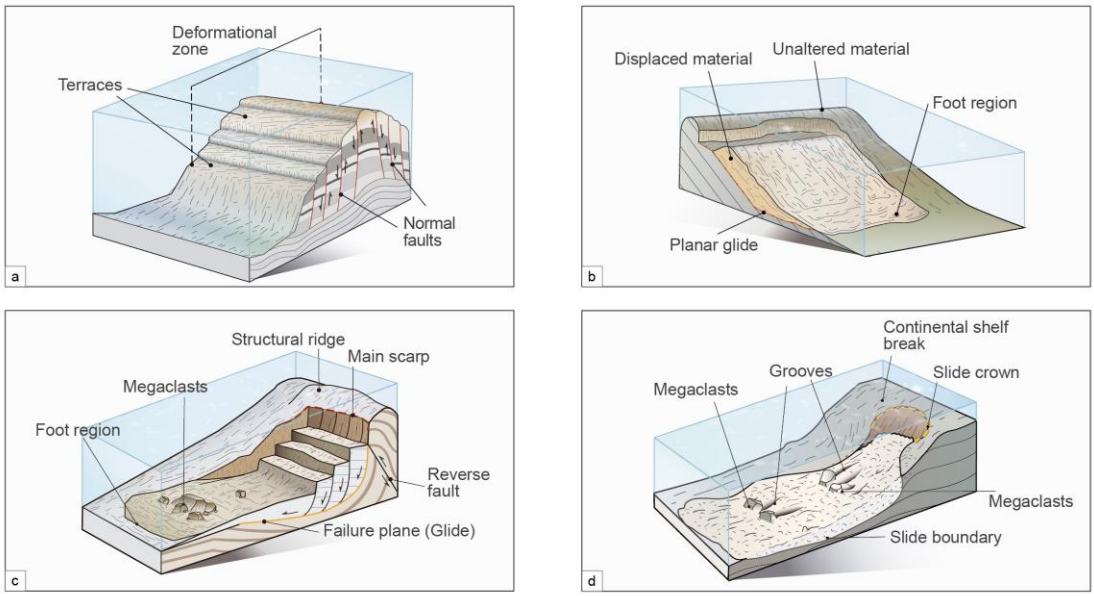

Figure 11. Processes that affect landslides. a) Deformational zones occur on structural ridge limbs and are interpreted like early stage of landslides. b) Translational slides occur when strong seismic reflector (bedding planes) concur with slope azimuth. c) Rotational slides occur where bedding dip azimuth is in opposite direction compared with slope azimuth. d) Debris flows occur at continental shelf break and feed MTCs on intra-slope sub-basins and abyssal plain.

Possible impact to future infrastructure

Preliminary observation of future infrastructure assessment hazards indicates that: i) Terrain T1 can generally be considered as low landslide hazard but movements could be triggered extreme events such as earthquakes. ii) T2 may be exposed to shallow displacements due to remobilization of MTCs as well as low energy parts of debris flows coming from T5. iii) In Terrain T3, displacements due to landslides, debris flows, and fault superficial ruptures should be considered for offshore structure design. iv) Terrain T4 may be exposed to landslides in the canyon and gully walls; v) T5 should be analyzed including the effect of debris flows originated at the

continental shelf break. vi) Risk of damage caused by rock falls or landslides increases in distances shorter than 4 km along structural ridges foothills in the whole study zone.

CONCLUSIONS

Based on seismic interpretation and seafloor morphological analyses 93 landslides were identified. These mass movement were grouped in 52 rotational slides, 29 translational slides and 12 complex landslides. In addition to landslides, 12 deformation zones and a mass transport complex (MTCs) zone were observed.

Rotational landslides reach horizontal displacements as long as 12.5 km thus being the longest ones for the whole study area. These displacements are linked to the SSDB thrust fault and structural ridges. They contribute in great manner to the filling of the intra-slope subbasins isolated from the continental shelf break. On the other hand, complex landslides involve areas exceeding 200 km^2 and in the same way as rotational landslides they are directly related to the SSDB structures and faults. The above suggests that most landslides in the study area come from tectonic movements inherent to SSDB evolution.

Debris flows consist of events mainly associated to the continental shelf break which involve non-cohesive sediments causing erosive scars (scours) on the seafloor, allowing to infer these landslide are the main feeder of MTCs found in intra-slope subbasins in terrain T5 and in the continental rise in terrain T2.

Five terrain types with different ground condition were defined from landslides distribution, geologic structures and seismic facies interpretation. Terrain type T1 is the flatter area in which morphology is dominated by low energy sedimentation supplied by the Magdalena rivers system. Terrain type T2 is a relative flat area (slope angle <5°) dominated by Mass Transport Complexes, this zone is feeded by the continental shelf break failure. Most landslides observed in this terrain type are located close to hill zones of the terrain type T3. Terrain type T3 is associated with North-East trend thrust faults beneath the SSFB. This region has the steepest hills, where the majority of landslides were identified. Terrain type T4, located to the southwest of the study region, close to Panama Plate edge, has steeped hills and small landslides. Terrain type T5 is formed by intra-slope subbasins filled by MTCs that over cross it and reach terrain type T2.

The main limitation for the understanding of submarine landslides in the study zone is due to the lack of information on the frequency of occurrence of different types of landslides. This would require the acquisition of new specialized data, such as: deep core piston, underwater vehicle campaigns (Gliders / AUV / ROV), seismic and high resolution bathymetry in different time periods as well as collecting dateable material to constrain the age of landsliding. These are key areas requiring further research to understand landslide risk in the South West Caribbean region.

ACKNOWLEDGEMENTS

This work was undertaken as part of Royal Academy of Engineering - Newton Fund grant IAPP1617/112 and the agreement FP44842-2017 Doctorado Empresa, ECOPETROL, EAFIT,

COLCIENCIAS (MINTIC). The data were kindly provided by Ecopetrol. Professors David Hodgson and Bill McCaffrey of the University of Leeds are acknowledged for discussion and advice.

REFERENCES

Alfaro, E., and M, Holz, 2014a, Seismic geomorphological analysis of deepwater gravity-driven deposits on a slope system of the southern Colombian Caribbean margin: Marine Petroleum Geology, **57**, 294–311. https://doi.org/10.1016/j.marpetgeo.2014.06.002

Bernal-Olaya, R., J. Sanchez, P. Mann, and M. Murphy, 2015, Along-strike Crustal Thickness Variations of the Subducting Caribbean Plate Produces Two Distinctive Styles of Thrusting in the Offshore South Caribbean Deformed Belt, Colombia, *in* C. Bartolini and P. Mann, eds., Petroleum Geology and Potential of the Colombian Caribbean Margin: AAPG Memoir **108**, p. 295–322. https://doi.org/10.1306/13531941M1083645

Bird, P., 2003, An updated digital model of plate boundaries: Geochemistry, Geophysics, Geosystems, **4**, 1-52. https://doi.org/10.1029/2001GC000252

Carter, L., J. D. Milliman, P. J. Talling, R. Gavey, and R. B. Wynn, 2012, Near-synchronous and delayed initiation of long run-out submarine sediment flows from a record-breaking river flood, offshore Taiwan: Geophys. Research Letters, **39**, 1-5. https://doi.org/10.1029/2012GL051172

Clare, M., J. Chaytor, O. Dabson, D. Gamboa, A. Georgiopoulou, H. Eady, J. Hunt, C. Jackson, O. Katz, S. Krastel, R. León, A. Micallef, J. Moernaut, R. Moriconi, L. Moscardelli, C. Mueller, A. Normandeau, M. Patacci, M. Steventon, M, Urlaub, D. Völker, L. Wood, and Z. Jobe, 2019, A consistent global approach for the morphometric characterization of subaqueous landslides: Geological Society, London, Special Publications, 477, 455-477. https://doi.org/10.1144/SP477.15

Cruden, D.M. and J. D. Varnes, 1996, Landslide types and procceses, *in* D. M. Cruden, D. J. Varnes, eds., Landslides: Investigation and Mitigation: Transportation Research Board Special Report.

Flinch, J.F., J. Amaral, A. Doulcet, B. Mouly, C. Osorio, and J.M. Pince, 2003, Structure of the Offshore Sinu Accretionary Wedge. Northern Colombia: 8th Simposio Bolivariano - Exploracion Petrolera en las Cuencas Subandinas, EAGE, Conference Proceedings, 76–83. https://doi.org/10.3997/2214-4609-pdb.33.Paper8

Green, A., and R. Uken, 2008, Submarine landsliding and canyon evolution on the northern KwaZulu-Natal continental shelf, South Africa, SW Indian Ocean: Marine Geology, **254**, 152–170. https://doi.org/10.1016/j.margeo.2008.06.001

Hampton, M A., H. J. Lee, and L. Jacques, 1996, Submarine landslides: Review of Geophysics, **34**, 35–59. https://doi.org/10.1029/95rg03287

He, Y., Zhong, G., Wang, L., Kuang, Z., 2014. Characteristics and occurrence of submarine canyon-associated landslides in the middle of the northern continental slope, South China Sea. Mar. Pet. Geol. https://doi.org/10.1016/j.marpetgeo.2014.07.003

Heidarzadeh, M., D. R. Tappin, and T. Ishibe, 2019, Modeling the large runup along a narrow segment of the Kaikoura coast, New Zealand following the November 2016 tsunami from a potential landslide: Ocean Engineering, **175**, 113–121. https://doi.org/10.1016/j.oceaneng.2019.02.024

Idárraga-García, J., D.G. Masson, J. García, H. León, and C.A. Vargas, 2019, Architecture and development of the Magdalena Submarine Fan (southwestern Caribbean): Marine Geology, **414**, 18–33. https://doi.org/10.1016/j.margeo.2019.05.005

Lamarche, G., J. Mountjoy, S. Bull, T. Hubble, S. Krastel, E. Lane, A. Micallef, L. Moscardelli, C. Mueller, I. Pecher, and S. Woelz, 2016, Submarine mass movements and their consequences: progress and challenges, *in* G. Lamarche, G., J. Mountjoy, S. Bull, T. Hubble, S. Krastel, E. Lane, A. Micallef, L. Moscardelli, C. Mueller, I. Pecher, and S. Woelz, eds., Submarine mass movements and their consequences – 7th International Symposium: Springer, **41**,1-13.

Leslie, S.C., and P. Mann, 2016, Giant submarine landslides on the Colombian margin and tsunami risk in the Caribbean Sea: Earth and Planetary Science Letters, **449**, 382–394. https://doi.org/10.1016/j.epsl.2016.05.040

Martinez, J.A., J. Castillo, A. Ortiz-Karpf, L. Rendon, J. C. Mosquera, and V. Vega, 2015, Deep water untested oil-play in the Magdalena Fan, Caribbean Colombian Basin, in: C. Bartolini, P. Mann, eds, Petroleum geology and potential of the Colombian Caribbean Margin. American Association of Petroleum Geologists, **108**, 251–260. https://doi.org/10.1306/13531955m1083658

Masson, D., C. Harbitz, R. Wynn, G. Pedersen, F. Løvholt, F, 2006, Submarine landslides: processes, triggers and hazard prediction. Philosophical Transactions of the Royal Society. A Mathematical, Physical and Engineering Sciences, **364**, 2009–2039. https://doi.org/10.1098/rsta.2006.1810

McAdoo, B.G., L.F. Pratson, and D.L. Orange, 2000, Submarine landslide geomorphology, US continental slope: Marine Geolology, **169**, 103-136. https://doi.org/10.1016/S0025-3227(00)00050-5

Moscardelli, L., and L. Wood, 2016, Morphometry of mass-transport deposits as a predictive tool: Bulletin of the Geological Society of America, **128**, 47–80. https://doi.org/10.1130/B31221.1

Moscardelli, L., L. Wood, and P. Mann, 2006, Mass-transport complexes and associated processes in the offshore area of Trinidad and Venezuela: American Association of Petroleum Geologist Bulletin, **7**, 1059–1088. https://doi.org/10.1306/02210605052

Nadim, F., O. Kjekstad, P. Peduzzi, C. Herold, and C. Jaedicke, 2006, Global landslide and avalanche hotspot: Landslides, **3**, 159–173. https://doi.org/10.1007/s10346-006-0036-1

Naranjo-Vesga, J., A. Ortiz-Karpf, L. Wood, Z. Jobe, J.F. Paniagua-Arroyave, L. Shumaker, D. Mateus-Tarazona, and P. Galindo, 2020, Regional controls in the distribution and morphometry of deep-water gravitational deposits along a convergent tectonic margin. Southern Caribbean of Colombia: Marine and Petroleum Geology, **121**, 1–30. https://doi.org/10.1016/j.marpetgeo.2020.104639

Ortiz-Karpf, A., D. M. Hodgson, C. A-L. Jackson, and W. D. McCaffrey, 2017, Influence of seabed morphology and substrate composition on mass-transport flow processes and pathways: Insights from the Magdalena Fan, Offshore Colombia: Journal of Sedimentary Research, **87**, 189–209. https://doi.org/10.2110/jsr.2017.10

Pindell, J.L., 1994, Evolution of the Gulf of Mexico and the Caribbean. Caribbean Geolology: An Introduction. 13–39.

Rincón, D. A., J. F. Naranjo, D. Mateus Tarazona, C. A. Hernández, H. D. Madero, J. De Bedout, A. Ortiz-Karpf, F. E. Malagón, and C. O. Cabrera, 2021, Geomorfología del fondo marino profundo en la región sur del caribe colombiano. Ecopetrol; Entrelibros. DOI: https://doi.org/10.29047/9789589287361

Rodríguez, I., M. Bulnes, J. Poblet, M. Masini, and J. Flinch, 2021, Structural style and evolution of the offshore portion of the Sinu Fold Belt (South Caribbean Deformed Belt) and adjacent part of the Colombian Basin: Marine and Petroleum Geology, **125**, 1-24. https://doi.org/10.1016/j.marpetgeo.2020.104862

Romero-Otero, G.A., 2009, Deepwater sedimentary processes in an active margin, Magdalena submarine fan, Offshore Colombia: PHD Thesis, University of Oklahoma.

Ruiz, C., N. Davis, P. Bentham, A. Price, and D. Carvajal, 2000, Structure and tectonic evolution of the South Caribbean Basin, Southern Offshore Colombia: a progressive accretionary prism: VII Simposio Bolivariano - Exploración Petrolera en las Cuencas Subandinas.

Shanmugam, G., 2016, Slides, slumps, debris flows, turbidity currents, and bottom currents: Reference Module in Earth Systems and Environmental Sciences. https://doi.org/10.1016/B978-0-12-409548-9.04380-3

Shanmugam, G. and Y. Wang, 2015, The landslide problem: Journal of Palaeogeogaphy, **4**, 109–166. https://doi.org/10.3724/SP.J.1261.2015.00071

Symithe, S., E. Calais, J.B. de Chabalier, R. Robertson, and M Higgins, 2015, Current block motions and strain accumulation on active faults in the Caribbean. Journal of Geophysical Research: Solid Earth, **120**, 3748–3774. https://doi.org/10.1002/2014JB011779

Tappin, D.R., P. Watts, G. M. McMurtry, Y. Lafoy, and T. Matsumoto, 2001, The Sissano, Papua New Guinea tsunami of July 1998 - Offshore evidence on the source mechanism: Marine Geolology, **175**, 1–23. https://doi.org/10.1016/S0025-3227(01)00131-1

Vanneste, M., C. F. Forsberg, S. Glimsdal, C.B. Harbitz, D. Issler, T. J. Kvalstad, F. Løvholt, and F. Nadim, 2013, Submarine landslides and their consequences: What do we know, what can we do?, *in* C. Margottini, P. Canuti, and K. Sassa, eds., Landslide Science and Practice - Complex Environment: Springer, **5**, 5–17. https://doi.org/10.1007/978-3-642-31427-8_1